Evaporation of Water and Uptake of HCl and HBr through Hexanol Films at the Surface of Supercooled Sulfuric Acid

Samuel V. Glass, Seong-Chan Park, and Gilbert M. Nathanson*

Department of Chemistry, University of Wisconsin—Madison, 1101 University Ave, Madison, Wisconsin 53706

Received: December 12, 2005; In Final Form: May 1, 2006

Vacuum evaporation and molecular beam scattering experiments have been used to monitor the loss of water and dissolution of HCl and HBr in deuterated sulfuric acid at 213 K containing 0 to 100 mM hexanol. The addition of 1-hexanol to the acid creates a surface film of hexyl species. This film becomes more compact with decreasing acidity, ranging from ∼62% to ∼68% of maximum packing on 68 to 56 wt % D_2SO_4, respectively. D_2O evaporation from 68 wt % acid remains unaltered by the hexyl film, where it is most porous, but is impeded by ∼20% from 56 and 60 wt % acid. H → D exchange experiments further indicate that the hexyl film on 68 wt % acid enhances conversion of HCl and HBr into DCl and DBr, which is interpreted as an increase in HCl and HBr entry into the bulk acid. For this permeable hexyl film, the hydroxyl groups of surface hexanol molecules may assist uptake by providing extra sites for HCl and HBr hydrogen bonding and dissociation. In contrast, HCl → DCl exchange in 60 wt % D_2SO_4 at first rises with hexyl surface coverage but then drops back to the bare acid value as the hexyl species pack more tightly. HCl entry is actually diminished by the hexyl film on 56 wt % acid, where the film is most compact. These experiments reveal a transition from a porous hexanol film on 68 wt % sulfuric acid that enhances HCl and HBr uptake to one on 56 wt % acid that slightly impedes HCl and D_2O transport.

Introduction

The transport of molecules between the ambient vapor and the liquid phase of aqueous aerosol droplets is an integral step in heterogeneous reactions in the atmosphere. Field measurements reveal that aqueous droplets in the upper troposphere contain significant quantities of organic molecules,[1] which may segregate to the surface of the particles and coat them.[2,3] Additional field studies provide direct evidence that aerosol particles in the lower troposphere, including aqueous sulfate aerosol, are coated with organic films.[4−6] These coatings have the potential to impede the rates of water evaporation and condensation and to impede gas uptake, thereby slowing droplet shrinkage and growth and altering the rates of chemical reactions that occur near the surface and in the bulk of these droplets.[2,3,7−9]

Multiphase processes in the atmosphere include reactions mediated by sulfuric acid aerosols that can contribute significantly to ozone depletion.[8,10,11] For example, HCl and HBr react with $ClONO_2$, $BrONO_2$, HOCl, and HOBr in sulfuric acid to produce Cl_2, Br_2, and BrCl. These molecules are then photolyzed by sunlight into halogen atoms that catalyze ozone destruction. While such reactions are most prevalent in the lower stratosphere, they also occur in the upper troposphere.[12−14] The rates of these heterogeneous reactions depend on the probability with which the impinging gas molecules enter the droplets,[15,16] and thus may be reduced by organic coatings. However, in order for this entry probability to be rate-limiting, a surfactant film must provide a significant reduction. For the reaction HCl(g) + HOBr(aq) → BrCl + H_2O in 60 and 70 wt % H_2SO_4 at 213 K, the HCl entry probability must drop below $\sim 10^{-4}$ in order to limit the overall rate of the bulk-phase reaction.[17,18] The limiting value for the analogous reaction of HBr rises to $\sim 10^{-2}$ because of the higher solubility (and longer residence time) of HBr in sulfuric acid solutions.[18−20]

Reductions in gas transport of this magnitude are indeed possible. Numerous experiments have shown that long-chain surfactants such as hexadecanol form compact monolayers on water at room temperature that can inhibit the rates of water evaporation and condensation by 4 or more orders of magnitude.[21] Do surfactants of this type exist in upper tropospheric aerosol particles? While the speciation is uncharacterized, there may be a wide variety of organics that can dissolve in or adsorb on aerosol particles, ranging from small molecules such as methanol and acetone to long-chain amphiphiles such as fatty acids.[1,3−6,22,23] Many laboratories have investigated reductions in gas transport posed by insoluble monolayers on water, but relatively little is known about the behavior of soluble surfactants in water or sulfuric acid.[24] A study of the surface structure and permeability of soluble surfactant films is essential to understand what is potentially occurring in aerosol droplets.

Gas transport through surface films depends strongly on the chain length of the surfactant. For alcohols and carboxylic acids, the resistance to gas permeation increases exponentially with chain length ranging from 14 to 22 carbon atoms.[21,25] The data are scarce for shorter-chain surfactants: several studies of slightly soluble surfactants with C_8−C_{12} alkyl chains show that these films do impede gas transport, but data is lacking to determine the chain length dependence.[24] An extrapolation of the data for C_{14}−C_{22} alcohols predicts that 1-butanol on water at 298 K would lower the rate of water evaporation by a factor of 100. However, experiments in our laboratory indicate that a film of butanol on 60 wt % D_2SO_4 at 213 K does *not* impede the evaporation of water and actually enhances the entry of HCl and HBr, even though the butyl surface coverage reaches ∼50% of maximum packing ($\sim 2.5 \times 10^{14}$ cm^{-2}).[26−28] In contrast, Thornton and Abbatt recently showed that N_2O_5 uptake is

* Corresponding author. E-mail: nathanson@chem.wisc.edu.

10.1021/jp057260t CCC: $33.50
Published on Web 05/28/2006

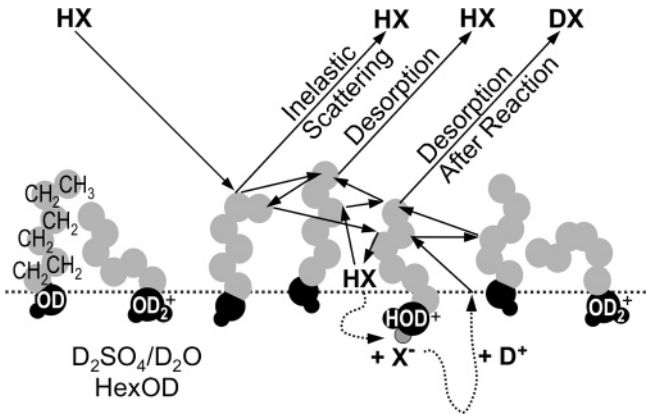

Figure 1. Several pathways for an HX molecule (X = Cl, Br) colliding with deuterated sulfuric acid containing 1-hexanol.

impeded threefold by hexanoic acid on sea salt aerosol at a surface concentration estimated to be 2×10^{14} cm^{-2}.[29] These different observations suggest that the rates of gas transport through surface films depend not only on the surfactant chain length and headgroup, but also on the gas molecule and underlying liquid.

The butanol studies indicate that this C_4 alcohol is too short to form a compact film on cold sulfuric acid that impedes water evaporation or HCl and HBr uptake.[30] As the chain length of the alcohol is increased above 4 carbon atoms, at what point does the film impose a resistance to the transport of protic gases? As a first step toward answering this question, we investigate here the effects of lengthening the alkyl chain by two CH_2 groups, from 1-butanol to 1-hexanol.

Consider HX (X = Cl or Br) molecules colliding with the surface of deuterated sulfuric acid coated with 1-hexanol, $CH_3(CH_2)_4CH_2OD$, as illustrated in Figure 1. The figure depicts a variety of hexyl chain configurations, motivated by simulations of short-chain alcohols on water that show diverse chain conformations at submonolayer coverages.[26,31,32] At thermal collision energies, nearly all impinging HX molecules will be momentarily trapped at the surface.[33,34] Some of these thermalized molecules may then be propelled into vacuum by thermal motions of the molecules at the surface before or after moving between the hexyl chains, while others may permeate fully through the film and enter the acid. To characterize these different processes, we measure the fraction f_{exch} of thermalized HX molecules that undergo H $\rightarrow$ D exchange and desorb as DX. We interpret f_{exch} to be the fraction of HX molecules that enter the bulk phase of the acid, either as intact HX or as X^- and H^+ after dissociating first in the interfacial region.[35] As discussed later, f_{exch} is strictly a lower limit to the entry probability, because some HX molecules that enter the acid may leave before dissociating. For the uncoated acid, we find that f_{exch} increases steadily as the acid is diluted, most likely because more D_2O become available in the near-interfacial region to act as hydrogen bonding and protonation sites for adsorbed HX molecules.[20,34]

The HX $\rightarrow$ DX exchange experiments described below show that this steady trend becomes more complex when the acid is coated with hexanol. We find that the permeability of the hexyl films, and their ability to enhance or inhibit gas transport, depends on the subphase acidity. At high acid concentrations, surface hexanol molecules enhance HX entry, perhaps by packing loosely enough to allow HX molecules facile access to the OD headgroups. Like interfacial D_2O, these OD headgroups may act as docking sites to help capture HCl and HBr that permeate through the hexyl chains. These chains become more compact at lower acidities, and assemble tightly enough to impede both D_2O evaporation and HCl entry.

Properties of Bare and Hexanol-Doped Sulfuric Acid

Table 1 lists properties of the three D_2SO_4 solutions used in the experiments, which are highly viscous and acidic and possess low water vapor pressures at 213 K. The acid dissociates extensively, consisting of D_2O, D_3O^+, DSO_4^-, and SO_4^{2-}.[36−39] 1-Hexanol (HexOD) dissolves in these acidic solutions up to at least 100 mM without freezing at 213 K (13 K below its bulk melting point). The acid reacts with the alcohol to produce $HexOD_2^+$ and hexylsulfuric acid (sulfate ester) $HexOSO_3D$,[40,41] which is strongly acidic and at least partially dissociated.[42] Studies of ethanol in sulfuric acid at 298 and 273 K in refs 43 and 44 can be combined to gauge the equilibrium concentrations of these species. In 58 wt % H_2SO_4, the equilibrium fractions are roughly 60% EtOH, 20% $EtOH_2^+$, and 20% $EtOSO_3H$/$EtOSO_3^-$, while in 70 wt % H_2SO_4, the fractions of EtOH, $EtOH_2^+$, and $EtOSO_3H/EtOSO_3^-$ are approximately equal. We expect that mixtures of HexOD in D_2SO_4 at 213 K will consist of these species as well, although the fraction of sulfate ester may be less than at equilibrium because of its slow formation rate.[41,44]

Surface tension measurements may be used to determine the total surface concentration of all hexyl species, which is equal to the Gibbs surface excess to within 1%.[47,49] Table 1 lists the hexyl surface concentrations extrapolated to 213 K from measurements at 295 and 250 K, which show that these hexyl species increasingly segregate to the surface of the acid at lower temperatures.[48] The values correspond to submonolayer coverages of 62%, 66%, and 68% of a compact film for 68, 60, and 56 wt % D_2SO_4, respectively. These fractions are based on a maximum surface density of 5×10^{14} cm^{-2} in which the alkyl chains are extended and close-packed.[50] The differences in packing for the three acid solutions are small, but the ordering at 295 and 250 K has been reproduced in each of 5 separate trials. This ordering might arise from increasing charge repulsion among neighboring $HexOD_2^+$ at higher acid concentrations.[47,51] The fraction of $HexOSO_3^-$ and $HexOSO_3D$ also grows with acid concentration, and these species should occupy more space at the surface than neutral HexOD.[52] Overall surface coverages of 62−68% imply that hexanol is very surface-active in sulfuric acid. For a 100 mM hexanol solution, the two-dimensional hexyl concentration in a cut through the bulk acid is only 2×10^{12} cm^{-2},[47] while the surface hexyl concentrations listed in Table 1 are ~150 times larger.

Experimental Procedure

Acid solutions are prepared by diluting 98 wt % D_2SO_4 with D_2O, adding 1-hexanol, and cooling to 213 ± 1 K in the Teflon reservoir depicted in Figure 2.[26] All reagents (Aldrich) are used without further purification. The surface tensions of the hexanol sample (≥99% purity) dissolved in water match literature values,[53] indicating that longer-chain species are not present.[48] Although we add HexOH rather than HexOD to the deuterated acid, the hydroxyl protons are scrambled throughout the acid and reduce the overall deuterium fraction by only 0.1 atom % at the highest hexanol concentration of 100 mM. Titrations indicate that the acid concentration changes by no more than 0.5 wt % during the time it is in vacuum (typically less than 5 days).[34]

A continuously renewed, vertical liquid surface is formed by rotation of a 5.0 cm diameter glass wheel partially submerged

TABLE 1: Comparison of Sulfuric Acid Solutions at 213 K Used in Experiments

D_2SO_4 formal concentration (wt %)	55.5	59.5	67.5
D_2SO_4 formal mole fraction	0.200	0.227	0.293
equivalent H_2SO_4 concentration (wt %)	57.6	61.5	69.3
equivalent H_2SO_4 molarity (M)[a]	9.0	9.9	11.8
viscosity (cP)[b]	300	470	1800
D_2O vapor pressure (Torr)[a]	1.6×10^{-3}	9.4×10^{-4}	2.4×10^{-4}
D^+ activity[a]	80	200	2000
hexyl surface coverage (10^{14} cm^{-2})[c,d]	3.4	3.3	3.1
(fraction of compact monolayer)	(~68%)	(~66%)	(~62%)

[a] Calculated from ref 38. [b] Calculated from refs 45 and 46. [c] Sum of all surface hexyl species, determined from surface tension measurements in refs 47 and 48. The surface coverage is roughly constant between 30 and 60 mM hexanol. [d] The relative uncertainty in the surface coverages is estimated to be less than $\pm 0.1 \times 10^{14}$ cm^{-2} based on the reproducibility of the 295 and 250 K measurements.

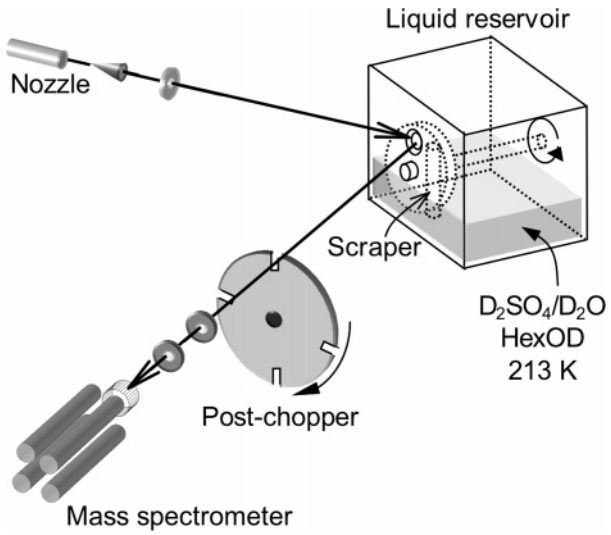

Figure 2. Diagram of the scattering apparatus and liquid reservoir. The Teflon reservoir is sealed except for a 0.9-cm-diameter hole through which the HX beam strikes the acid.

in 60 mL of the acid solution (see Figure 2).[26,34] The coated wheel is skimmed by a cylindrical Teflon scraper, which removes the outer 0.1 cm of acid. The remaining ~0.05-cm-thick acid film then passes in front of a 0.7 cm^2 circular hole, where it is intercepted by the impinging molecular beam. At a typical wheel speed of 0.17 Hz, the time between scraping and appearance at the edge of the hole is 0.49 s. Argon scattering and hexanol evaporation measurements show that this replenishment time allows the hexyl film to be fully reestablished at the surface of the acid, in accord with previous measurements for butanol.[54] The acid then remains in front of the hole for 0.49 s and is exposed to the beam for 0.27 s.

Beams of 90 kJ mol^{-1} Ar, 100 kJ mol^{-1} HCl, and 150 kJ mol^{-1} HBr are generated by expanding a 2% mixture of each species in H_2 through a 0.13-mm-diameter glass nozzle at ~1 bar total pressure. A beam of 150 kJ mol^{-1} CF_3CH_2OH is also created by bubbling H_2 through the neat liquid held at 8.0 °C.[27] Each beam is directed at the acid at an incident angle $\theta_{inc} = 45°$, projecting a 0.36 cm × 0.51 cm elliptical spot. Molecules scattering or desorbing from the acid are detected by a mass spectrometer at $\theta_{fin} = 45°$. The molecules strike the acid continuously, and the exiting species are chopped into 36 μs pulses. Their arrival times at the mass spectrometer are measured over a flight path of 19.0 cm. The mass spectrometer detects the different species at $m/z = 20$ (D_2O), 31 and 32 (CF_3CH_2OH and CF_3CH_2OD monitored at CH_3O^+ and CH_2DO^+), 38 and 39 (HCl and DCl), 40 (Ar), and 82 and 83 (HBr and DBr).

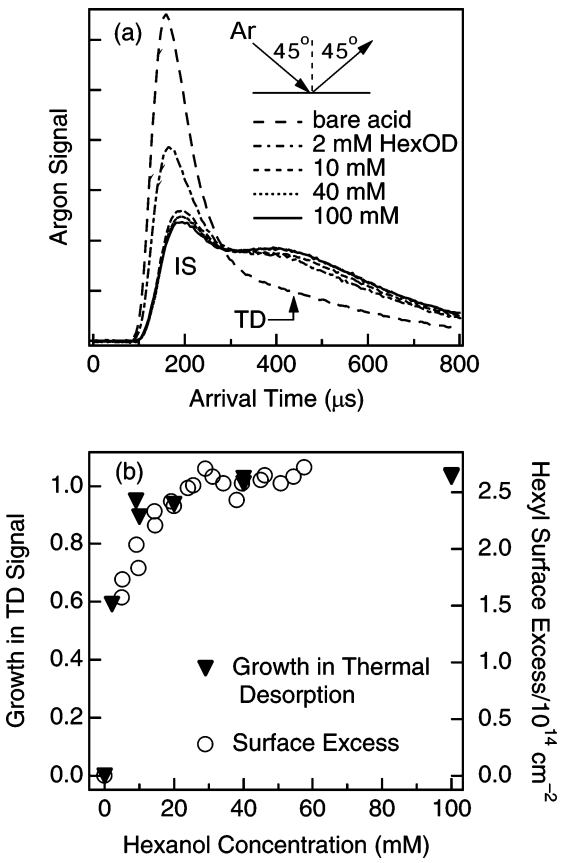

Figure 3. (a) TOF spectra of 90 kJ mol^{-1} Ar scattering from 68 wt % D_2SO_4 at 213 K containing 0, 2, 10, 40, and 100 mM 1-hexanol (HexOD). "IS" and "TD" refer to direct inelastic scattering and trapping−desorption. (b) Fractional increase in the Ar TD signal (▼) versus bulk HexOD concentration. The surface concentration of hexyl species (○), calculated from surface tension measurements in 69 wt % H_2SO_4 at 295 K, is plotted against the right-hand axis.[48] The asymptotic concentration at 213 K rises to ~3.1×10^{14} cm^{-2}.

Results and Analysis

Hyperthermal Argon Scattering from Bare and Hexanol-Doped 56−68 wt % D_2SO_4. Coupled surface tension and argon scattering measurements provide a direct way to characterize the packing of the surface hexyl species on the acid in vacuum.[26] Figure 3a shows time-of-flight (TOF) spectra of argon atoms following collisions at $E_{inc} = 90$ kJ mol^{-1} (50 RT_{acid}) and $\theta_{inc} = 45°$ with 68 wt % D_2SO_4 at 213 K containing 0−100 mM HexOD. The bare acid spectrum displays two components stemming from distinct pathways that Ar atoms follow upon colliding with the surface. The narrow peak at early arrival times (high exit velocities) corresponds to those atoms that undergo direct inelastic scattering (IS), transferring on average 70% of

their incident energy to the acid during one or a few collisions before recoiling away. The broader peak at later arrival times (lower exit velocities) corresponds to Ar atoms that become momentarily trapped in the interfacial region and then thermally desorb (TD). This region of the spectrum can be fit with a Maxwell−Boltzmann distribution at the acid temperature of 213 K (not shown).[26]

The TOF spectra change dramatically when the acid is doped with 1-hexanol. As the hexanol concentration is increased from 0 to 100 mM, the IS component sharply diminishes in intensity and shifts to later arrival times. These changes indicate that fewer Ar atoms scatter at the specular angle and that those Ar atoms that do scatter transfer more of their incident energy to the surface before recoiling away. Concurrently, the thermal desorption (TD) signal grows upon addition of HexOD, indicating that more Ar atoms thermalize on the surface with increasing hexanol concentration. The Ar spectra change most dramatically between bare acid and 20 mM HexOD, and only small differences occur at higher concentrations.

The changes in the argon IS and TD components mirror changes in the surface concentration of hexyl species. Figure 3b displays the fractional increase in TD intensity relative to bare acid, $(I_{TD}^{HexOD} - I_{TD}^{bare})/I_{TD}^{bare}$, versus bulk hexanol concentration. On the right-hand axis is plotted the hexyl surface concentration, shown here for 69 wt % H_2SO_4 at 295 K.[48] The surface coverage follows a Langmuir-type adsorption curve, rising rapidly at low bulk hexanol concentrations and then plateauing near 20 mM. Panel b confirms that the growth in argon TD signal tracks the hexyl surface coverage. We find that the decrease in IS intensity and shift in energy transfer (not shown) also track the hexyl surface concentration; these trends are also observed for 56 and 60 wt % D_2SO_4.[54]

The trends in Ar scattering are consistent with our previous results for butanol in Figure 4 of ref 26, which also show a correlation between the argon scattering patterns discussed above and the surface coverage of butyl species. We argued that the growth in thermal desorption, reduction in inelastic scattering, and shift in energy transfer are best explained by the increased roughening of the surface and the reduced effective surface mass when alkyl groups coat the surface.[26,33] The similarity between the trends in Ar scattering and the surface excess curves of butanol and hexanol provides strong evidence that the surface concentration is the same when the film is prepared using a continuously renewed, vertical surface in vacuum and when using a static, horizontal surface in air.

Evaporation of Water from Bare and Hexanol-Doped 56−68 wt % D_2SO_4. Figure 4a compares TOF spectra of D_2O evaporation from solutions of 56, 60, and 68 wt % D_2SO_4 containing 0 and 40 mM HexOD. These spectra show that the added hexanol reduces the D_2O evaporation signal from the 56 and 60 wt % D_2SO_4 solutions but has no effect on evaporation from 68 wt % D_2SO_4. This behavior differs significantly from our previous studies of butanol in 60−68 wt % D_2SO_4: in 60 wt % D_2SO_4, hexanol *does impede* D_2O evaporation, whereas butanol does *not*.[26] However, in 68 wt % D_2SO_4, the hexyl surface film, like the butyl film, is fully permeable. These differences are highlighted further in the lower panel, which displays the normalized D_2O evaporation flux as a function of hexanol concentration in the 56 and 60 wt % D_2SO_4 solutions. For hexanol concentrations of 10 mM and higher, the D_2O evaporation flux is 75−85% of the flux from bare acid.

Collisions of HCl with Bare and Hexanol-Doped 56−68 wt % D_2SO_4. Figure 5a shows TOF spectra of HCl and DCl following collisions of 100 kJ mol^{-1} HCl with 68 wt % D_2SO_4 at 213 K. The HCl spectrum is composed of HCl molecules that scatter directly and those that thermalize and then desorb. A fraction f_{exch} of the thermalized HCl molecules also undergo H → D exchange and then desorb as DCl. Both HCl and DCl thermal desorption signals are fit well by Maxwell−Boltzmann curves at 213 K. The fraction f_{exch} is calculated from

$$f_{exch} = \frac{I_{TD}^{DCl}}{I_{TD}^{DCl} + I_{TD}^{HCl}} \quad (1)$$

where I_{TD} is the relative flux of thermally desorbing molecules obtained from each TOF spectrum. The measured exchange fraction from Figure 5a is 0.14 ±0.03 for 68 wt % D_2SO_4 at 213 K; approximately one out of seven HCl molecules that thermalize on the surface undergoes H → D exchange and desorbs as DCl, while the remaining HCl desorb before reacting. The ±0.03 error bar reflects one standard deviation in reproducibility of ±0.02 and an estimated ±0.01 uncertainty in fitting the TD components. The value of $f_{exch} = 0.14$ agrees well with previous measurements,[20,27,34] which also showed that f_{exch} is independent of incident energy for values of 100, 47, and 14 kJ mol^{-1}. Beam reflectivity measurements further indicate that fewer than 1% of the thermalized HCl molecules do not desorb from the acid during the 0.5 s time that the liquid is exposed to the vacuum, in accord with the 50 μs average residence time of DCl in 68 wt % D_2SO_4 at 213 K.[34] Therefore, the DCl flux in eq 1 does not need to be corrected for molecules remaining in the acid.[55]

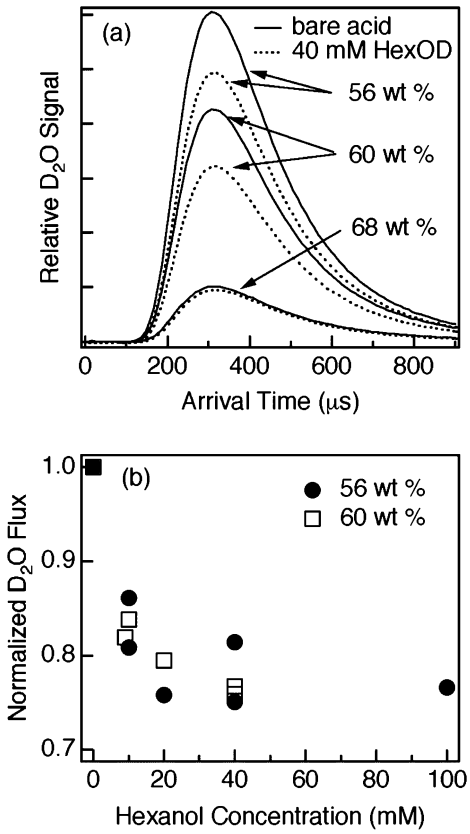

Figure 4. (a) TOF spectra of D_2O evaporation from 56, 60, and 68 wt % D_2SO_4 containing 0 and 40 mM HexOD. These spectra reveal that the hexyl film impedes D_2O evaporation from 56 and 60 wt % D_2SO_4 but not from 68 wt % acid. (b) D_2O evaporation flux versus hexanol concentration in 56 and 60 wt % D_2SO_4 at 213 K, normalized at 0 mM HexOD. The uncertainty in the fluxes is ±5%. The ratios of the bare acid signals agree with ratios of the predicted D_2O vapor pressures to within 15%.[38]

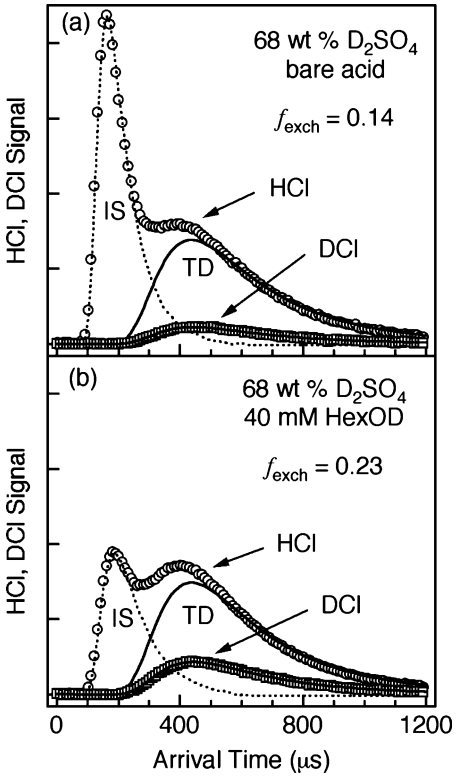

Figure 5. TOF spectra of HCl and H → D exchanged DCl following collisions of 100 kJ mol^{-1} HCl with 68 wt % D_2SO_4 at 213 K containing (a) 0 and (b) 40 mM HexOD. The HCl IS channel is represented by the dotted curve, and the HCl and DCl TD components are fit by Maxwell−Boltzmann distributions (solid curves). The spectra are displayed on the same vertical axis in each panel.

The effects of doping the 68 wt % D_2SO_4 solution with 40 mM HexOD are displayed in Figure 5b. The inelastic scattering intensity is suppressed, and the IS peak is shifted to slightly later arrival times. These trends are identical to those observed for argon atom collisions shown in Figure 3a, as well as for HCl collisions with 60−68 wt % D_2SO_4 containing butanol.[27] The value of f_{exch} is 0.23 in 68 wt % acid, obtained from the HCl and DCl TD components according to eq 1. This value is *larger* than that for bare acid (0.14) and slightly less than the value of 0.27 measured with 68 wt % D_2SO_4 containing 0.18 M BuOD.[27]

Figure 6 captures our most important results for HCl → DCl exchange with hexyl-coated sulfuric acid. Panel a shows that in 68 wt % D_2SO_4 the f_{exch} values mirror the trend in the surface segregation of hexyl species: f_{exch} increases sharply at low hexanol concentrations before approaching an asymptotic value characteristic of a Langmuir adsorption curve. As in Figure 3b, the hexyl surface excess is plotted against the right-hand axis, calculated from surface tension measurements of hexanol in 69 wt % H_2SO_4 at 295 K.[48] The similar trends in f_{exch} and hexyl surface coverage imply that changes in H → D exchange with the addition of hexanol are caused by the presence of hexyl species at the surface rather than by hexyl species dissolved in the bulk.

We observe qualitatively different behavior for HCl in 60 and 56 wt % D_2SO_4, as shown in Figure 6b and c. In 60 wt % acid (panel b), f_{exch} rises sharply at low hexanol concentrations but at higher concentrations falls back to the bare acid value. In 56 wt % acid (panel c), after an initial small rise at 2 mM HexOD, the HCl exchange fraction decreases steadily, dropping from the bare acid value of 0.68 to a final value of 0.59. These trends disappear when hexanol is replaced by butanol: f_{exch} instead rises by 0.1 in 56 wt % acid and 0.2 in 60 wt % acid as the butanol concentration is increased from 0 to 0.18 M, and the butyl surface coverage rises to ∼50% of maximum packing.[27,28,56] As discussed later, the addition of hexanol to 56 wt % D_2SO_4 marks our first observation that a soluble surfactant can actually impede the entry of HCl into sulfuric acid.

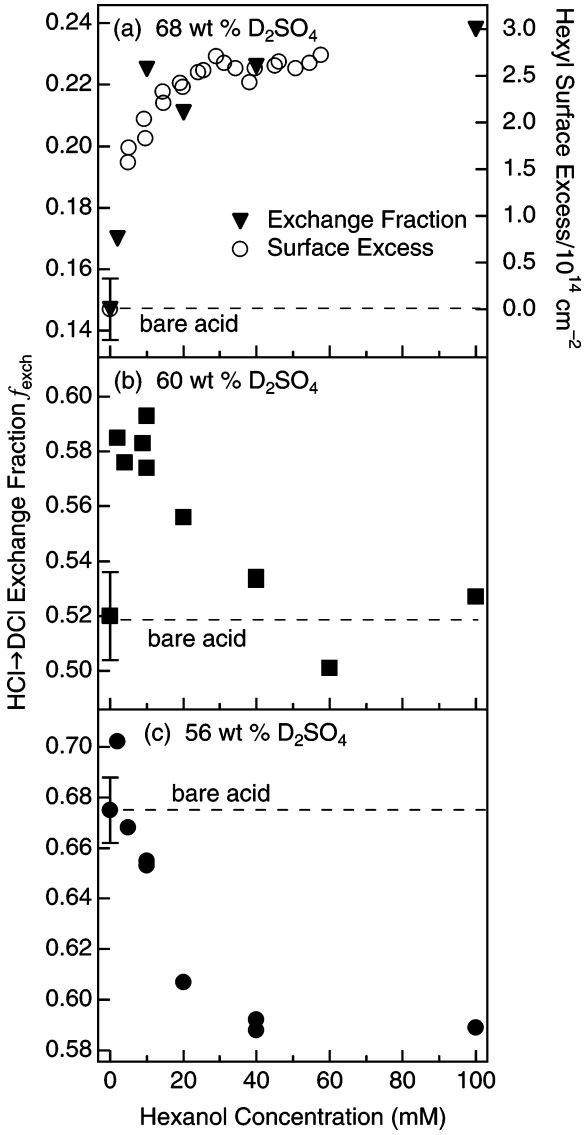

Figure 6. HCl → DCl exchange fraction f_{exch} versus HexOD concentration in (a) 68 wt %, (b) 60 wt %, and (c) 56 wt % D_2SO_4 at 213 K. The error bars for the bare acid represent ±1 σ in f_{exch} for 3, 8, and 4 measurements, respectively, in panels a, b, and c. The hexyl surface concentration is plotted in (a) for 69 wt % H_2SO_4 at 295 K. The three panels depict how the hexyl film undergoes a transition from enhancing H → D exchange in (a) to impeding exchange in (c).

Collisions of HBr with Bare and Hexanol-Doped 68 wt % D_2SO_4. Figure 7 shows the dependence of HBr → DBr exchange on hexanol concentration in 68 wt % D_2SO_4 at 213 K (left-hand axis) together with the surface excess of hexyl species (right-hand axis). Upon addition of hexanol, f_{exch} rises to 0.63, an increase of more than twofold from the bare acid value of 0.29. Just as with HCl in Figure 6a, the HBr f_{exch} values track the surface segregation of hexyl species. Experiments with HBr were not conducted in more dilute solutions because its bulk-phase residence time exceeds the time of the measurement, making it difficult to account for all HBr species that enter the solution.

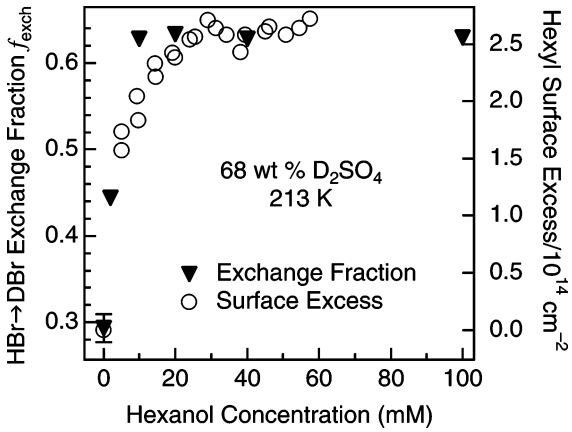

Figure 7. H → D exchange fraction versus hexanol concentration for thermalized HBr following collisions at $E_{inc} = 150$ kJ mol^{-1} with 68 wt % D_2SO_4 at 213 K. The hexyl surface concentration at 295 K is plotted against the right-hand axis.

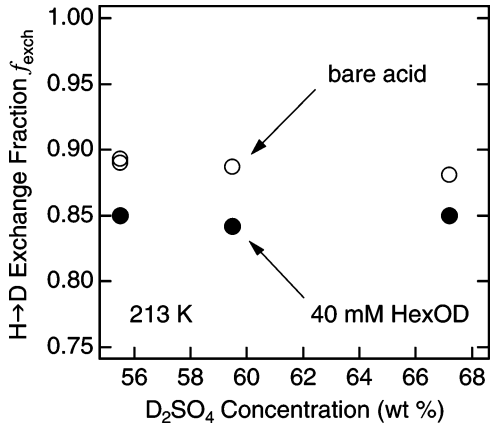

Figure 8. H → D exchange fraction versus D_2SO_4 concentration at 213 K for thermalized CF_3CH_2OH following collisions at $E_{inc} = 150$ kJ mol^{-1} with 0 and 40 mM HexOD.

Collisions of CF_3CH_2OH with Bare and Hexanol-Doped 56−68 wt % D_2SO_4. 2,2,2-Trifluoroethanol (TFE) is a strongly hydrogen bonding molecule that, unlike HCl and HBr, is easily protonated in sulfuric acid solutions. Previous measurements confirm that its solubility is low enough that almost all of the dissolved TFE evaporates within the observation time of 0.5 s.[27] Figure 8 shows the values of f_{exch} following collisions of 150 kJ mol^{-1} TFE with 56, 60, and 68 wt % D_2SO_4 containing 0 and 40 mM hexanol. The exchange fractions are independent of acid concentration over the 12 wt % range, in contrast to the behavior observed for HCl and HBr. The value of f_{exch} drops from 0.89 for bare acid to 0.85 for 40 mM HexOD, a change that is just bracketed by the experimental uncertainty. These results are very similar to those obtained with butanol[27] and indicate that nearly all thermalized TFE molecules undergo H → D exchange and then desorb as CF_3CH_2OD.

Discussion

The water evaporation and H → D exchange experiments indicate that a hexyl film on sulfuric acid may enhance or impede gas transport, depending on the concentrations of the acid and hexanol and on the identity of the solute. We argue below that this complex behavior stems from the compactness of the hexyl film and the availability of interfacial D_2O and HexOD protonation sites, which vary with both hexanol concentration and subphase acidity.

Evaporation of Water. The D_2O evaporation spectra in Figure 4 reveal that hexyl films impede water evaporation from 56 and 60 wt % D_2SO_4 but not from 68 wt % D_2SO_4. The unimpeded evaporation of D_2O from 68 wt % D_2SO_4 solutions coated with hexyl films parallels our previous study,[26] which demonstrated that butanol films on 60−68 wt % D_2SO_4 do not alter water evaporation. This unimpeded evaporation implies that, at equilibrium, the condensation of water must also be unaltered by the hexyl film. The entry probability of water into bare 68 wt % D_2SO_4 at 213 K is predicted to be close to 1.[57] For the hexyl-coated acid, this implies that almost all water molecules impinging on the surface at thermal energies enter the bulk acid. From the perspective of a water molecule in the gas phase, the hexyl film on 68 wt % D_2SO_4 appears porous and sticky: gaps between the hexyl chains allow the D_2O molecule to move through the surface film, while the attractive forces between D_2O and the hexyl chains and polar headgroups draw the water molecule into the acid before it can evaporate.

The onset of a surfactant barrier to water evaporation is observed when the acidity of the subphase is lowered from 68 to 60 wt % D_2SO_4. The ∼20% reduction in the evaporation rate of D_2O in Figure 4 implies that the hexyl film is more compact on 60 wt % than on 68 wt % D_2SO_4. This is in accord with the increase in surface coverage from 62% to 66% of a compact monolayer on 68 to 60 wt % acid. For comparison, a 4% increase in surface coverage of hexadecanol on water near maximum packing reduces water evaporation by fourfold.[21] Related experiments by Rubel with hexadecanol films on phosphoric acid also indicate that the transport of water through the film decreases at lower acidities.[58] The author hypothesized that this trend originates from charge repulsion between neighboring protonated hexadecanol molecules, which inhibits close packing at the surface. As mentioned earlier, this explanation, along with increasing sulfation of the alcohol, should also be responsible for the slightly looser packing of hexyl species at higher sulfuric acid concentrations.[47,52]

There are at least two mechanisms by which the hexyl chains can assemble at the surface to impose a barrier to water evaporation.[21] The film may be relatively uniform, allowing most water molecules to pass through fluctuating gaps between the chains but occasionally hindering some, or it may be heterogeneous, composed of more tightly clustered islands surrounded by permeable regions of lower density. Monte Carlo simulations of a 1-hexanol film on water, constrained to be close-packed at 5×10^{14} cm^{-2}, show that the hydroxyl groups form hydrogen bonds with water molecules and with each other, but also show that the penetration of water molecules beyond the hydroxyl groups is negligible.[59] This impermeability is in contrast to a Monte Carlo simulation of butanol on water,[31] in which the lower surface coverage of 4×10^{14} cm^{-2} results in a more disordered, porous film that allows water molecules to penetrate between the alkyl chains. Sum frequency studies indicate that water molecules can be detected even between decanol molecules on water at the same coverage of 4×10^{14} cm^{-2}.[60] The butanol simulations further reveal that some butanol molecules cluster and shift vertically, opening up more bare surface than if the chains had assembled at the same height.[26] Although this clustering is small and likely short-lived for butanol on water at 298 K, it may be more extended and longer-lasting for hexanol on sulfuric acid at 213 K.[61] Thus, transient openings between individual chains and larger-scale regions of different densities may both contribute to the overall porosity of the cold hexyl film.

Control of Gas Uptake by Hexyl Films. The trends in the HX → DX exchange fraction f_{exch} for HCl and HBr further delineate changes in the permeability of the hexyl film with subphase acidity. They also provide direct evidence for acid−base interactions between adsorbed HX molecules and the OD groups of surface hexanol.

The discussion below rests in part on the association of f_{exch} with the fraction β of HX molecules that enter the acid at thermal collision energies either as HX or as X^- and H^+.[35] In two previous studies, we used pulsed molecular beams to investigate this association for HCl and HBr entering uncoated acid.[20,34] HCl and HBr that emerge as DCl and DBr dissolve as neutral species or ions for long times (average residence times of 10^{-5} to 10^{+1} s for 68 to 56 wt % D_2SO_4 at 213 K). In contrast, HCl and HBr molecules that do not undergo exchange spend on average less than 10^{-6} s in the acid, the shortest measurable time in our experiments. The actual time may be much shorter, and we interpret it to imply that these HX molecules desorb from the surface before dissolving into the bulk region of the acid. This 10^{-6} s upper limit corresponds to an average diffusion distance of $(D\tau)^{1/2} < 10$ Å using a bulk phase diffusion coefficient D of 10^{-8} cm^2 s^{-1},[62] equivalent to a depth of 2−3 molecular layers. It is possible that some HX molecules diffuse fully into the bulk and then return to the surface and evaporate before undergoing H → D exchange. In this case, the entry probability β would be larger than f_{exch}. Our inability to interrogate gas−liquid interactions at times shorter than 1 μs prohibits us from investigating the fate of HCl and HBr at a finer atomic scale. We can therefore only equate β and f_{exch} within the assumption that the contact time between the acid and HX molecules that do not undergo exchange is short enough that they do not diffuse into the bulk region of the acid before evaporating.

This H → D exchange analysis was first applied to HCl and HBr collisions with uncoated 70 to 55 wt % D_2SO_4 at 213 K. Ref 20 shows that f_{exch} increases from 0.1 to 0.7 for HCl and 0.2 to 0.9 for HBr as the acid is diluted. This trend was explained by postulating that the addition of D_2O to the acid provides extra interfacial sites for HCl and HBr hydrogen bonding and dissociation. More recent studies show that HBr molecules that do not undergo exchange with butyl-coated acid are again characterized by average solvation times shorter than 10^{-6} s, while those that undergo H → D exchange dissolve in the acid on average for 4×10^{-4} s in 68 wt % D_2SO_4.[27] These distinct time scales indicate that β may also be equated with f_{exch} in the presence of a surfactant film under the assumption stated above. This equality is also consistent for HCl collisions with butyl-coated acid, but the residence times for DCl/Cl^- in the acid were short enough that we cannot rule out the possibility that some HCl → DCl exchange occurs within the butyl film itself, followed by immediate DCl desorption.[27] Additional pulsed-beam experiments yield identical conclusions for HBr and HCl collisions with hexyl-coated acid.[56] Given the similarity between HCl and HBr—strongly acidic gases that hydrogen bond to and protonate D_2O, BuOD, and HexOD—it seems reasonable to assume that nearly all HCl molecules that undergo exchange must also dissolve in the butyl and hexyl-coated acids (as HCl, Cl^- and H^+, or DCl) before desorbing as DCl.

Within this analysis, the enhanced passage of HCl and HBr through the hexyl film and into 68 wt % D_2SO_4 in Figures 6a and 7 is consistent with the observation in Figure 4 that water evaporation is unimpeded. The HCl and HBr entry probabilities initially rise sharply at low hexanol concentrations and then plateau at higher concentrations, in parallel with the hexyl surface coverage. We argued for butyl-coated acid that these trends are consistent with a picture in which the basic OD groups of the alcohol act as hydrogen-bonding sites that assist HX molecules in dissolving into the acid or as protonation sites that initiate dissociation at the film−acid interface. The same trends observed here for hexanol support this argument: interfacial OD headgroups facilitate the entry of HCl and HBr, while the hexyl chains are packed loosely enough on 68 wt % acid to allow these molecules to pass between the hexyl chains.

The hexyl film becomes more compact as the acid concentration is lowered from 68 to 60 wt % D_2SO_4, as shown by the onset of resistance to water evaporation (Figure 4) and by surface tension measurements that yield an increase in surface coverage from 62% to 66% of a compact monolayer.[48] As depicted in Figure 6b, f_{exch} rises by ∼0.06 at low hexanol concentrations but falls back down to the bare acid value at higher concentrations. We attribute the enhancement at low coverages to facile access of the surface hexanol OD groups to HCl. At higher hexanol concentrations, the surface film becomes more compact and hinders a fraction of the HCl molecules from reaching the hexanol OD groups. The equal entry probabilities for bare and hexyl-coated acid at saturation is likely accidental, arising because the enhanced entry caused by extra OD groups at the surface is countered by a reduction in transport due to the tighter packing of the hexyl chains. Our surface tension measurements are unfortunately not precise enough to determine the hexyl coverage at which this turnover occurs, and we can only say that the asymptotic surface coverage rises from ∼3.1 to $\sim 3.3 \times 10^{14}$ cm^{-2} as the acid is diluted from 68 to 60 wt % D_2SO_4.

The cancellation between enhanced entry caused by basic OD headgroups and reduced entry caused by chain packing occurs at very low hexanol concentrations in 56 wt % acid, between 2 and 5 mM, where the surface coverage has not yet reached saturation. At higher concentrations, the hexyl film becomes compact enough to impede HCl entry. Figure 6c shows a reduction from 0.68 to 0.59 at the highest coverage of ∼68% of a compact monolayer, or ∼2% more compact than on 60 wt % acid. At this lowest acidity, the film is least porous, and the HCl molecules are not able to reach interfacial D_2O or hexanol OD groups as often because of the more tightly packed chains.

The minimal reduction in entry of CF_3CH_2OH shown in Figure 8 stands in contrast to observed changes for HCl and D_2O. In the case of butyl-coated acid, which does not impede water evaporation, we argued that the nearly unimpeded TFE entry could be explained by the porosity of the butyl film and by the facile protonation of TFE in the interfacial region. The hexyl film, however, does reduce D_2O evaporation by ∼20% in 56 wt % D_2SO_4. TFE may be less impeded by the organic film because it is more polarizable (∼6 Å^3) than HCl (2.7 Å^3) or D_2O (1.3 Å^3).[63] As it is composed of both nonpolar and basic groups, TFE may interact strongly enough with the hexyl chains[64] to be drawn into the acid and react with near-interfacial D_3O^+ on almost every encounter.

Atmospheric Implications and Conclusions

The most striking result from the present studies is the transition from a porous and completely permeable hexyl film on 68 wt % D_2SO_4 to a film on 60 and 56 wt % D_2SO_4 that impedes gas transport. The D_2O evaporation experiments yield equal evaporation rates from bare and hexyl-coated 68 wt % D_2SO_4, analogous to our previous measurements of butyl-coated 60−68 wt % D_2SO_4.[26] The high acidity of the subphase most likely causes the film to expand as more $HexOD_2^+$ repel each

other and as more HexOD are converted to $HexOSO_3D$/$HexOSO_3^-$. The onset of resistance to water evaporation (~20% reduction for 56 and 60 wt % D_2SO_4) is likely caused by tighter packing of the hexyl chains when the acid concentration is lowered. This onset can be considered alternately from the perspective of the alkyl chain length: on 60 wt % D_2SO_4 at 213 K, the resistance to water evaporation commences with chain lengths between 4 and 6 carbon atoms.

The amphiphilic nature of hexanol allows it to catalyze or impede HCl → DCl exchange, depending on the hexyl surface packing and subphase acidity. We associate these changes in exchange probability with changes in the entry of HCl into the acid, either as intact HCl or as Cl^- and H^+ after dissociating first in the interfacial region. Within this interpretation, we find that interfacial hexanol molecules raise the entry probability of HCl and HBr into 68 wt % D_2SO_4 from 0.14 to 0.23 for HCl and from 0.29 to 0.63 for HBr, values similar to those observed with butanol films.[27] This increase in uptake is likely due to the OD groups of loosely packed alcohol molecules, which provide extra interfacial hydrogen bonding and protonation sites that assist HX dissociation. In 60 wt % D_2SO_4, the HCl entry probability rises from 0.52 to 0.58 at low hexanol concentrations, but at higher concentrations, the tighter packing of hexyl chains at the surface cancels this enhancement. The HCl entry probability into 56 wt % D_2SO_4 is actually reduced from 0.68 to 0.59 by the more compact hexyl film, an effect that does not occur with the shorter-chain butyl film.[56]

Our results imply that hexanol films can reduce the rates of water evaporation and condensation into supercooled sulfuric acid droplets, but will not limit reactions of HCl or HBr with dissolved HOCl or HOBr, which would occur only if the entry probability dropped below $\sim 10^{-4}$ for HCl or $\sim 10^{-2}$ for HBr.[18] The transition from a barrierless butanol layer to a slightly impermeable hexanol layer suggests that much longer-chain alcohols may assemble tightly enough to achieve dramatic reductions in the transport of HCl, HBr, or H_2O into supercooled sulfuric acid.[65] This trend may be closely accompanied by a transition from soluble surfactants to insoluble ones, which should display even richer conformational behavior than observed here for 1-hexanol as a function of surface coverge.[66,67]

Acknowledgment. We are grateful to the Air Force Office of Scientific Research for supporting this work and to the Camille and Henry Dreyfus Foundation for providing a postdoctoral fellowship in environmental chemistry to S.-C. P. We also thank James Krier for surface tension measurements and David Hanson and Akihiro Morita for valuable discussions.

References and Notes

(1) Murphy, D. M.; Thomson, D. S.; Mahoney, T. M. J. *Science* **1998**, *282*, 1664.

(2) Ellison, G. B.; Tuck, A. F.; Vaida, V. *J. Geophys. Res. Atmos.* **1999**, *104*, 11633.

(3) Gill, P. S.; Graedel, T. E.; Weschler, C. J. *Rev. Geophys. Space Phys.* **1983**, *21*, 903.

(4) Russell, L. M.; Maria, S. F.; Myneni, S. C. B. *Geophys. Res. Lett.* **2002**, *29*, 1779.

(5) Tervahattu, H.; Juhanoja, J.; Kupiainen, K. *J. Geophys. Res. Atmos.* **2002**, *107*, 4319.

(6) Tervahattu, H.; Juhanoja, J.; Vaida, V.; Tuck, A. F.; Niemi, J. V.; Kupiainen, K.; Kulmala, M.; Vehkamaki, H. *J. Geophys. Res. Atmos.* **2005**, *110*, D06207.

(7) Rudich, Y. *Chem. Rev.* **2003**, *103*, 5097.

(8) Finlayson-Pitts, B. J.; Pitts, J. N. *Chemistry of the Upper and Lower Atmosphere*; Academic Press: New York, 2000; Chapters 9.C and 12.C.

(9) Vieceli, J.; Ma, O. L.; Tobias, D. J. *J. Phys. Chem. A* **2004**, *108*, 5806.

(10) For studies of ozone in the stratosphere and troposphere, see Jacob, D. *Atmos. Environ.* **2000**, *34*, 2131. Solomon, S. *Rev. Geophys.* **1999**, *37*, 275. Staehelin, J.; Harris, N. R. P.; Appenzeller, C.; Eberhard, J. *Rev. Geophys.* **2001**, *39*, 231. Fahey, D. W.; Kawa, S. R.; Woodbridge, E. L.; Tin, P.; Wilson, J. C.; Jonsson, H. H.; Dye, J. E.; Baumgardner, D.; Borrmann, S.; Toohey, D. W.; Avallone, L. M.; Proffitt, M. H.; Margitan, J.; Loewenstein, M.; Podolske, J. R.; Salawitch, R. J.; Wofsy, S. C.; Ko, M. K. W.; Anderson, D. E.; Schoeberl, M. R.; Chan, K. R. *Nature (London)* **1993**, *363*, 509.

(11) For laboratory investigations of heterogeneous reactions in sulfuric acid, see Donaldson, D. J.; Ravishankara, A. R.; Hanson, D. R. *J. Phys. Chem. A* **1997**, *101*, 4717. Shi, Q.; Jayne, J. T.; Kolb, C. E.; Worsnop, D. R.; Davidovits, P. *J. Geophys. Res. Atmos.* **2001**, *106*, 24259. Waschewsky, G. C. G.; Abbatt, J. P. D. *J. Phys. Chem. A* **1999**, *103*, 5312. Leu, M. T. *Int. Rev. Phys. Chem.* **2003**, *22*, 341.

(12) Hendricks, J.; Lippert, E.; Petry, H.; Ebel, A. *J. Geophys. Res. Atmos.* **1999**, *104*, 5531.

(13) Karcher, B.; Solomon, S. *J. Geophys. Res. Atmos.* **1999**, *104*, 27441.

(14) Meilinger, S. K.; Karcher, B.; von Kulmann, R.; Peter, T. *Geophys. Res. Lett.* **2001**, *28*, 515.

(15) Hanson, D. R. *J. Phys. Chem. B* **1997**, *101*, 4998.

(16) Worsnop, D. R.; Morris, J. W.; Shi, Q.; Davidovits, P.; Kolb, C. E. *Geophys. Res. Lett.* **2002**, *29*, 1996.

(17) Waschewsky, G. C. G.; Abbatt, J. P. D. *J. Phys. Chem. A* **1999**, *103*, 5312.

(18) Hanson, D. R. *J. Geophys. Res. Atmos.* **2003**, *108*, 4239.

(19) Abbatt, J. P. D.; Nowak, J. B. *J. Phys. Chem. A* **1997**, *101*, 2131.

(20) Behr, P.; Morris, J. R.; Antman, M. D.; Ringeisen, B. R.; Splan, J. R.; Nathanson, G. M. *Geophys. Res. Lett.* **2001**, *28*, 1961.

(21) Barnes, G. T. *Colloids Surf., A* **1997**, *126*, 149.

(22) Singh, H.; Chen, Y.; Tabazadeh, A.; Fukui, Y.; Bey, I.; Yantosca, R.; Jacob, D.; Arnold, F.; Wohlfrom, K.; Atlas, E.; Flocke, F.; Blake, D.; Blake, N.; Heikes, B.; Snow, J.; Talbot, R.; Gergory, G.; Sachse, G.; Vay, S.; Kondo, Y. *J. Geophys. Res. Atmos.* **2000**, *105*, 3795.

(23) Singh, H.; Chen, Y.; Staudt, A.; Jacob, D.; Blake, D.; Heikes, B.; Snow, J. *Nature (London)* **2001**, *410*, 1078.

(24) For a review of gas transport through surfactant films, see the introduction of ref 26.

(25) La Mer, V. K.; Healy, T. W.; Aylmore, L. A. G. *J. Colloid Sci.* **1964**, *19*, 673.

(26) Lawrence, J. R.; Glass, S. V.; Nathanson, G. M. *J. Phys. Chem. A* **2005**, *109*, 7449.

(27) Lawrence, J. R.; Glass, S. V.; Park, S.-C.; Nathanson, G. M. *J. Phys. Chem. A* **2005**, *109*, 7458.

(28) The surface concentration of butyl species at 0.18 M butanol was estimated in ref 26 to be 80% of maximum packing (4×10^{14} cm^{-2}) on 60 wt % D_2SO_4 at 213 K. New measurements in ref 48 show that the surface coverage is closer to 50%.

(29) Thornton, J. A.; Abbatt, J. P. D. *J. Phys. Chem. A* **2005**, *109*, 10004.

(30) See also Morita, A. *Chem. Phys. Lett.* **2003**, *375*, 1, for simulations showing that methanol enters unimpeded into methanol-coated water.

(31) Chen, B.; Siepmann, J. I.; Klein, M. L. *J. Am. Chem. Soc.* **2002**, *124*, 12232.

(32) Daiguji, H. *Microscale Thermophys. Eng.* **2002**, *6*, 223.

(33) Nathanson, G. M. *Annu. Rev. Phys. Chem.* **2004**, *55*, 231.

(34) Morris, J. M.; Behr, P.; Antman, M. D.; Ringeisen, B. R.; Splan, J.; Nathanson, G. M. *J. Phys. Chem. A* **2000**, *104*, 6738.

(35) The overall entry probability β differs from the mass accommodation coefficient α, which is the fraction of molecules entering the liquid in the absence of surface reactions. β instead refers to the bulk-phase entry of HX into the acid in all of its possible forms, including HX, X^- and H^+ ion pairs, or separated ions, DX, and $XOSO_3^-$. As emphasized in ref 15, α is not a useful parameter when some of the gas molecules react first at the surface, and we should not have used this variable in refs 27 and 34 to label HCl and HBr entry into sulfuric acid. The α notation is common in the literature, however, when it is unclear whether molecules enter the bulk intact or after reacting in the interfacial region.

(36) Chen, H.; Irish, D. E. *J. Phys. Chem.* **1971**, *75*, 2672.

(37) Myhre, C. E. L.; Christensen, D. H.; Nicolaisen, F. M.; Nielsen, C. J. *J. Phys. Chem. A* **2003**, *107*, 1979.

(38) Carslaw, K. S.; Clegg, S. L.; Brimblecombe, P. *J. Phys. Chem.* **1995**, *99*, 11557. Carslaw, K. S.; Peter, T.; Clegg, S. L. *Rev. Geophys.* **1997**, *35*, 125. Calculations were performed at mae.ucdavis.edu/wexler/aim.htm.

(39) See also Bianco, R.; Wang, S.; Hynes, J. T. *J. Phys. Chem. B* **2005**, *109*, 21313 for the possible existence of molecular H_2SO_4 at the surface of sulfuric acid.

(40) Deno, N. C.; Newman, M. S. *J. Am. Chem. Soc.* **1950**, *72*, 3852.

(41) Iraci, L. T.; Essin, A. M.; Golden, D. M. *J. Phys. Chem. A* **2002**, *106*, 4054.

(42) Heathcock, C. H.; Streitwieser, A. *Introduction to Organic Chemistry*, 4th ed.; MacMillan: New York, 1992.

(43) Clark, D. J.; Williams, G. *J. Chem. Soc.* **1957**, 4218.

(44) Lee, D. G.; Cameron, R. *J. Am. Chem. Soc.* **1971**, *93*, 4724.

(45) Williams, L. R.; Long, F. S. *J. Phys. Chem.* **1995**, *99*, 3748.

(46) Klenø, J. G.; Kristiansen, M. W.; Nielsen, C. J.; Pedersen, E. J.; Williams, L. R.; Pedersen, T. *J. Phys. Chem. A* **2001**, *105*, 8440.

(47) Torn, R. D.; Nathanson, G. M. *J. Phys. Chem. B* **2002**, *106*, 8064.

(48) Krier, J. M.; Nathanson, G. M. To be submitted for publication.

(49) For studies of 1-hexanol films on ice, see Sokolov, O.; Abbatt, J. P. D. *J. Phys. Chem. A* **2002**, *106*, 775.

(50) Kaganer, V. M.; Möhwald, H.; Dutta, P. *Rev. Mod. Phys.* **1999**, *71*, 779.

(51) Rubel, G. O.; Gentry, J. W. *J. Phys. Chem.* **1984**, *88*, 3142.

(52) The hexyl groups may also bend toward the surface at higher acid concentrations if the alkyl chains are more attracted to interfacial sulfate species than to D_2O. This greater attraction may be driven by the higher polarizabilities of DSO_4^- (6 Å^3), SO_4^{2-} (7 Å^3), and D_2SO_4 (5 Å^3) than of D_2O (1.3 Å^3). See Jungwirth, P.; Curtus, J. E.; Tobias, D. J. *Chem. Phys. Lett.* **2003**, *367*, 704, for SO_4^{2-} and Jungwirth, P. for unpublished estimates for bisulfate and sulfuric acid.

(53) Li, Z. X.; Lu, J. R.; Thomas, R. K.; Rennie, A. R.; Penfold, J. *J. Chem. Soc., Faraday Trans.* **1996**, *92*, 565.

(54) Glass, S. V. Ph.D. Thesis, University of Wisconsin—Madison, 2005.

(55) The correction to f_{exch} for net gas uptake γ during the measurement time is given by $f_{exch} = I_{TD}^{DCl}/(I_{TD}^{DCl} + I_{TD}^{HCl}(1 - \gamma/\beta))$, where β is the entry probability. For the experiments reported here, the correction due to γ increases f_{exch} by less than 0.01 for HCl and 0.02 for HBr. These small corrections have not been applied to the tabulated values of f_{exch} obtained from eq 1.

(56) Park, S.-C.; Glass, S. V.; Nathanson, G. M. To be submitted for publication. This article will explore detailed-balance constraints on the connection between HCl solvation times and entry probabilities in surfactant-coated sulfuric acid.

(57) Gershenzon, M.; Davidovits, P.; Williams, L. R.; Shi, Q. A.; Jayne, J. T.; Kolb, C. E.; Worsnop, D. R. *J. Phys. Chem. A* **2004**, *108*, 1567. Figure 3 predicts that the entry probability of H_2O into 70 wt % H_2SO_4 at 213 K should exceed 0.9.

(58) Rubel, G. O. *J. Phys. Chem.* **1987**, *91*, 2103.

(59) Gao, J.; Jorgenson, W. L. *J. Phys. Chem.* **1988**, *92*, 5813.

(60) Tyrode, E.; Johnson, C. M.; Kumpulainen, A.; Rutland, M. W.; Claesson, P. M. *J. Am. Chem. Soc.* **2005**, *127*, 16848.

(61) Simulations of model six-atom soluble surfactants in an atomic liquid depict this surface patchiness even more clearly. See Tomassone, M. S.; Couzis, A.; Maldarelli, C. M.; Banavar, J. R.; Koplik, J. *J. Chem. Phys.* **2001**, *115*, 8634.

(62) Klassen, J. K.; Hu, Z. J.; Williams, L. R. *J. Geophys. Res. Atmos.* **1998**, *103*, 16197.

(63) The ~6 Å^3 polarizability for CF_3CH_2OH was estimated from the values of 4.4 for CF_3CH_3 and 1.5 for H_2O.

(64) Mmereki, B. T.; Chaudhuri, S. R.; Donaldson, D. J. *J. Phys. Chem. A* **2003**, *107*, 2264.

(65) The entry probability of HCl into pure 1-octanol droplets is only 0.008 at 273 K, suggesting that this surfactant may significantly impede HCl uptake into sulfuric acid. In contrast, the more polarizable and more acidic HBr molecule enters 1-octanol on each collision. See Zhang, H. Z.; Li, Y. Q.; Davidovits, P.; Williams, L. R.; Jayne, J. T.; Kolb, C. E.; Worsnop, D. R. *J. Phys. Chem. A* **2003**, *107*, 6398.

(66) Gaines, G. L. *Insoluble Monolayers at Liquid−Gas Interfaces*; Interscience Publishers: New York, 1966.

(67) Gilman, J. B.; Eliason, T. L.; Fast, A.; Vaida, V. *J. Colloid Interface Sci.* **2004**, *280*, 234.